POINT MEASUREMENT OF DETONATION WAVE PROPAGATION USING ION GAUGE

by

NITESH KARPAKALA MANJUNATHA GUPTA

Presented to the Faculty of the Graduate School of
The University of Texas at Arlington in Partial Fulfillment
of the Requirements
for the Degree of

MASTERS IN MECHANICAL ENGINEERING

THE UNIVERSITY OF TEXAS AT ARLINGTON

December 2013

Dedicated to my family and friends

ACKNOWLEDGEMENTS

First, I would like to thank my supervising professors Dr.Donald Wilson and Dr.Frank Lu without whom this thesis would not have been possible. I thank them for their constant support, guidance, inspiration and the opportunity to work at the Aerodynamics Research Center which kept me going till the end. I am extremely grateful to Dr. Luca Maddalena, my committee member who has given his invaluable time, and shown interest in my thesis.

Special thanks go to David Carter, who helped with the facility modifications and his assistance to ensure that the experiments were conducted safely. I would further like to thank all my colleagues, Dibesh Joshi, Andrew Mizener, Adrian Muller, Sarah Hussein and Raheem Bello at the ARC who have constantly helped me, and supported me at different times during my presence in this lab. It was always a pleasure working with them in the lab. I would like to thank all my friends, Sriram Srinivasan, Rohit Sridharan and Madhukar Shanbag who have constantly helped and supported me throughout my masters. Their support, belief, and encouragement always gave me a moral boost and always kept me going.

Finally I would like the express my fullest gratitude to my beloved parents for always believing in me and supporting me at all times.

November 22, 2013

ABSTRACT

POINT MEASUREMENT OF DETONATION WAVE PROPAGATION USING ION GAUGE

Nitesh Karpakala Manjunatha Gupta, M.S.

The University of Texas at Arlington, 2013

Co-Supervising Professors: Dr. Donald Wilson and Dr. Frank Lu

Accurate measurement of detonation wave velocity is important in the study of detonations. Detonation wave velocity is calculated by the ratio of distance between two transducers which the wave front travels over to the propagation time. Conventional methods included transducers placed a few cm apart thereby yielding an average velocity of the wave. A gauge was developed in which the transducers were placed a few mm apart so that an effective point measurement of velocity can be determined.

Different types of sensors used in determining the detonation wave velocity included pressure, flame and ion. Of the three, the ion sensor was chosen because of its simple and straightforward mechanical and electrical design, and compactness. A pair of ion gauges was built into a four-hole ceramic tube potted with epoxy into a steel plug. Solid copper wires were used as electrode pairs. The distance between the two gauges was around 5.2 mm thereby giving a point measurement. A non-stationary cross-correlation technique was then used to determine the velocity and its uncertainty.

The technique was tested in a 2-in. ID and 30-ft long stainless steel detonation tube. Five ion gauges were installed along the length of the tube. The results were compared against those obtained from pressure transducers spaced 60 in. apart.

TABLE OF CONTENTS

ACKNOWLEDGEMENTS iv

ABSTRACT v

LIST OF ILLUSTRATIONS ix

Chapter Page

1. INTRODUCTION 1

1.1 Objective 2

1.2 Background 2

1.2.1 Detonations 2

1.2.2 Cross Correlation 4

2. METHODOLOGY 7

2.1 Development and Testing of Ion Gauge 7

2.1.1 Operation of Ion Gauge 7

2.1.2 Sensor Development 8

2.1.3 Testing of Ion Gauge 9

2.2 Detonation Tube 11

2.2.1 Data Acquisition 13

2.2.2 Detonation Tube Operation 15

3. RESULTS AND DISCUSSION 17

3.1 Results of Ion Gauge Testing 17

3.2 Results from Detonation Tube 20

3.2.1 Results from NASA CEA Code 21

3.2.2 Experimental Results 21

3.2.3 Shock Tube Experiments 26
4. CONCLUSIONS AND FUTURE WORK 33
4.1 Conclusions 33
4.2 Future Work 33
Appendix
A. Cross Correlation Code 35
REFERENCES 40
BIOGRAPHICAL STATEMENT 42

LIST OF ILLUSTRATIONS

Figure		Page
1.1	ZND model for detonation wave	4
1.2	Example for two waves considered for cross correlation [1]	5
1.3	Enlargement of the wave fronts [1]	6
2.1	Circuit for ion gauge, [2]	8
2.2	Ion gauge	9
2.3	Detonation tube (dimensions in mm)	10
2.4	Test section showing pressure transducers and ion gauge	11
2.5	Panoramic view of shock-induced detonation tube	12
2.6	Detonation tube with data acquisition	14
3.1	Pressure transducer outputs	17
3.2	Ion gauge outputs	18
3.3	Nonstationary cross-correlation of the ion gauge	19
3.4	Propagating velocities of detonation wave	20
3.5	PCB pressure output for 3 atm	22
3.6	Ion gauge output for 3 atm	23
3.7	Ion gauge output from oscilloscope	24
3.8	Cross correlation plot for ion gauge 2	25
3.9	Velocity profile for 2 atm	26
3.10	Velocity profile for 3 atm	27
3.11	Velocity profile for 2 atm (repeatability)	27
3.12	PCB pressure output for 2 atm	28

3.13 Velocity from pressure transducer for 2 atm 29
3.14 Velocity from pressure transducer for 3 atm 30
3.15 Pressure ratio along the tube for 2 atm 30
3.16 Pressure ratio along the tube for 3 atm 31
3.17 Comparison with Mirel's theory for 2 atm 32
3.18 Comparison with Mirel's theory for 3 atm 32

CHAPTER 1

INTRODUCTION

Over the years, studies have been made to understand the behavior of detonation wave phenomenon propagating in a tube [3, 4]. The Velocity of a detonation wave in a tube provides information on the deflagration-to-detonation transition length, the strength of the wave and its attenuation behavior. This information helps in designing detonation-based engines. Hence, accurate measurement of detonation wave velocity is very important. A pair of transducers, spaced a distance of Δx is used to measure the time taken for the wave to travel is Δt. Thus the detonation velocity is

$$U_D = \frac{\Delta x}{\Delta t} \tag{1.1}$$

This is known as the time-of-flight method. Practically, a pair of sensors can be placed a few cm apart. Placing the sensors at this distance has at least two main limitations. First, velocity obtained is the average between the two sensors. This averaging process creates uncertainty if the wave speed is changing either due to viscous drag or due to deflagration-to-detonation transition. The time-of-flight method, the traditional way of determining the velocity between two sensors, does not account for uncertainty. This difficulty compromises the ability to provide an uncertainty estimate to the velocity which can be a problem when comparing different data sets. Secondly, having the sensors few cm apart is not satisfactory, since we are interested in determining the velocity at a point [1]. To satisfy this, Δx has to be very small. This requirement creates additional complications. The above equation (1.1) shows that a very small Δx and the high speed of the detonation wave combined yeild a very small time delay. To detect this small time delay, we a need very high-speed data acquisition system.

1.1 Objective

Attenuation of shock wave was studied to understand its behavior [5] and studies have been made in a shock-induced detonation tube.This research is divided into two parts. The first part is on developing and testing of ion gauges to yield a point velocity measurement. The second part is on using multiple ion gauges and pressure transducers to study detonation wave propagation through a tube. The detonation wave is accomplished by igniting an oxy-hydrogen mixture with a shock wave. Velocities were determined using the time-of-flight method and the cross-correlation technique. Six pressure transducers and five ion sensors were mounted along the tube to obtain wave propagation data.

1.2 Background

1.2.1 Detonations

'A detonation wave is essentially a shock supported by a trailing exothermic reaction.' A detonation wave is a combustion wave propagating at supersonic speed whereas a deflagration is a combustion wave propagating at subsonic speed.

Generally, two modes of initiations exist in detonations, one which is known by thermal initiation where transition occurs from deflagrations and the other where initiation occurs due to an ignition blast or a shock wave. In the former case, i.e., in thermal initiation, the burned gases from the initial deflagration have a specific volume which is 5–15 times that of the unburned gases. Since each compression wave that results from this deflagration heats the unburned gases ahead of this wave to an extent, the sound velocity increases and succeeding waves catch up to the initial one. This process continues to preheat the unburned gases. This sequence of events leads to a shock and thus a detonation wave is formed. This transition

length from deflagration to detonation is of the order of a meter. In the case of ignition blast, detonation can only occur when a strong shock wave is generated by a source. Under these conditions *"the blast and reaction front are always coupled in the form of a multiheaded detonation wave that starts at the source and expands at about the detonation velocity"*[6]. Hence, the reaction rate plays an important role in establishing a detonation wave.

Chapman and Jouguet were the first to propose a theory that permitted a mathematical solution for the detonation velocity. They assumed the detonation wave to be steady, planar and one-dimensional. This theory is called the Chapman–Jouguet theory. Once the detonation velocity is known, the final state of the products can be determined. They also proposed that for these conditions, the flow behind the supersonic detonation wave is sonic based on local thermodynamic state. This point on the Hugonoit curve is called the upper C-J point and other conditions in this state are called C-J conditions. However, this theory does not provide the transition from initial to final state across the wave. A detailed model specifies the transition from one state to another. This model is called the ZND (Zeldovich–von Neumann–Döring) model.

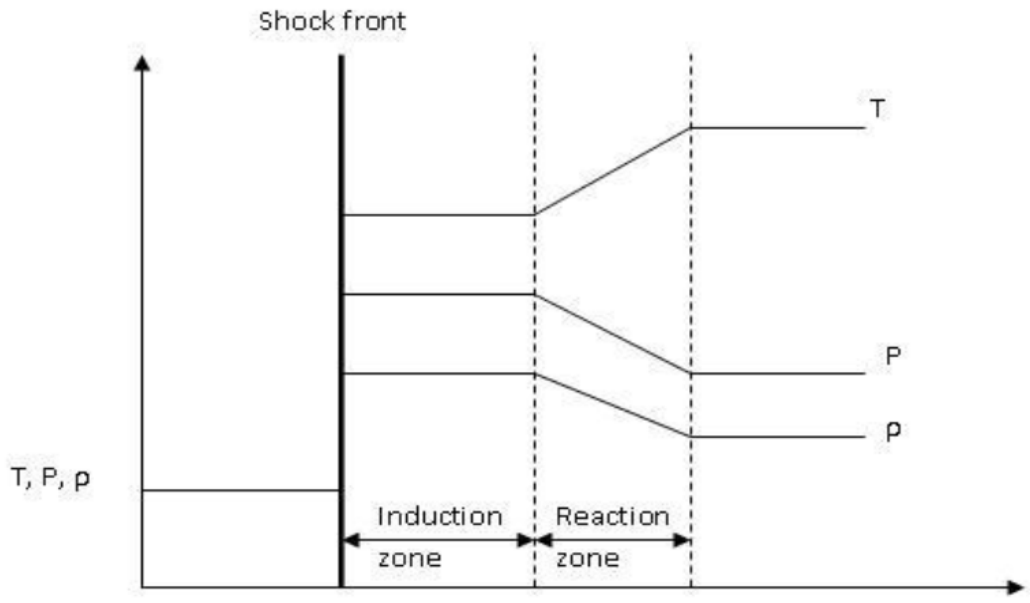

Figure 1.1. ZND model for detonation wave.

Figure 1.1 shows a sketch of ZND model. This ZND model consists of a shock front that adiabatically compresses the gas ahead of it, thus heating up the molecules. The induction zone follows this front where the species at their ignition temperature are dissociated to form radicals and at this point the thermodynamic properties are almost constant. Finally, rapid chemical energy release in the reaction zone drives the front forward. Thus, in the ZND model of detonation, both the ignition and driving mechanism are specified.

1.2.2 Cross Correlation

Cross correlation is the extent of similarity between two waveforms as a function of time lag applied to them. The time-of-flight (TOF) method has been much used to determine the time delay between two waveforms. But this method becomes less

powerful when it comes to shock and detonation waves as the waves are arbitrary in nature. In such situations, cross correlation becomes a powerful tool. It not only gives an estimate of time delay between two waveforms, but also gives an uncertainty in the time delay estimate [1]. Cross correlations can be extended to non-stationary waveforms.

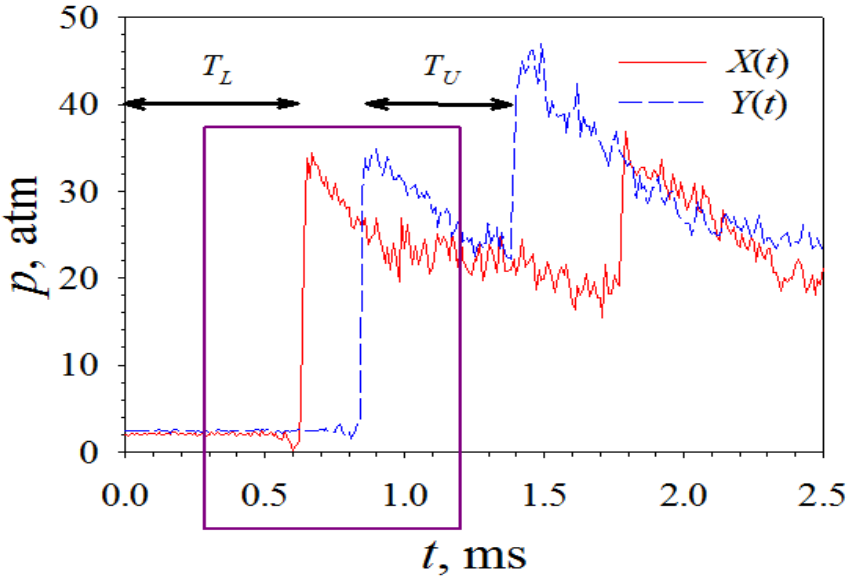

Figure 1.2. Example for two waves considered for cross correlation [1].

Figure 1.2 shows an example of two waves considered for applying cross correlation. T_L and T_U are the ranges of the lower and upper limits of the integration window. After applying cross correlation between the two signals, the maximum of the cross correlation function provides the propagation time.

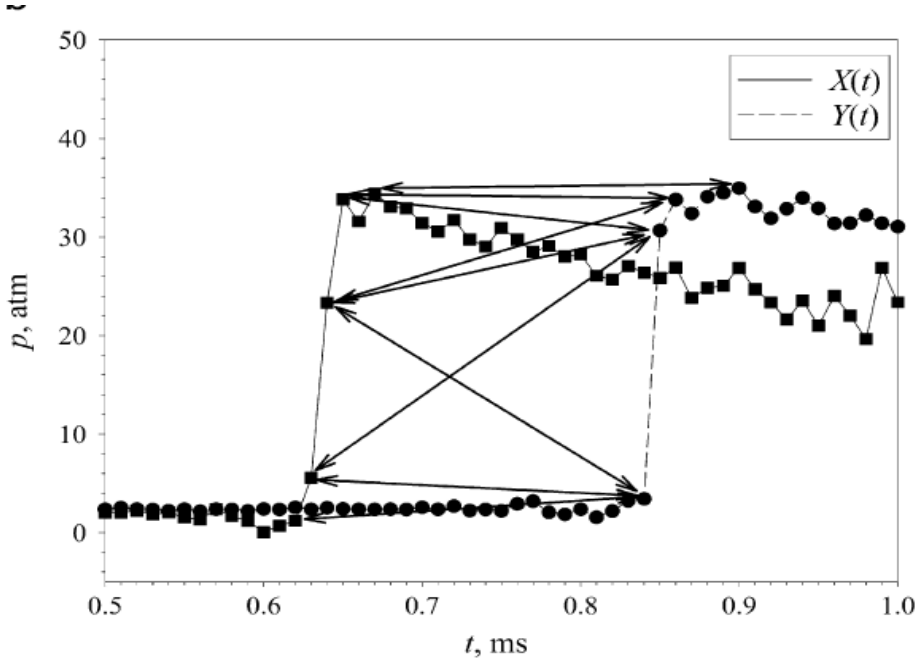

Figure 1.3. Enlargement of the wave fronts [1].

Figure 1.3 shows the zoomed in version of the wave fronts. The double-headed arrows indicate possible pairs of data points for the TOF method, resulting in estimates of uncertainty. Wavelets and spectral methods can also be used to determine the time delay between the waves [7, 8]

CHAPTER 2

METHODOLOGY

2.1 Development and Testing of Ion Gauge

2.1.1 Operation of Ion Gauge

Figure 2.1 shows the circuit used for the ion gauge. The ion gauge works on the principle that the high conductivity of the gases in the detonation wave closes the circuit through the probe [2]. This discharges the capacitor C_1 through the resistors R_1 . The time constant for recharging the capacitor is determined by the R_2C_1 [9]. The values of R_2 and C_1 are chosen in such a way that the recharge time is around 5 μs. This recharging of the capacitor helps in detecting multiple waves.

The resistance between the two terminals in a probe are high. To overcome this resistance, high voltage is supplied for to create an ionized path for the current to flow.

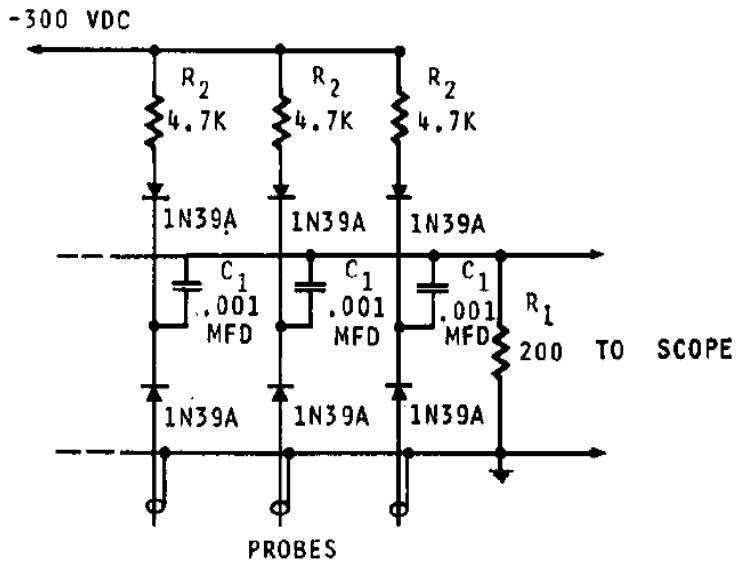

Figure 2.1. Circuit for ion gauge, [2].

2.1.2 Sensor Development

As shown in fig.2.2, two ion gauges were built in a stainless steel 1/4th-inch NPT plug. The distance between them was 5.2 $\pm$ 0.05 mm. A pair of two-hole ceramic tubes of 8 cm in diameter was used to house the electrodes. The electrodes were made of solid copper wires of 18AWG (1.2 mm). A frame was made to house the electrodes, ceramic tubes and the stainless steel plug. The ceramic tubes were then potted using an epoxy sealant (JB weld) into the stainless steel plug. The epoxy takes 12–14 hours to harden. Finally, excess sealant was sanded to smoothen the surface.

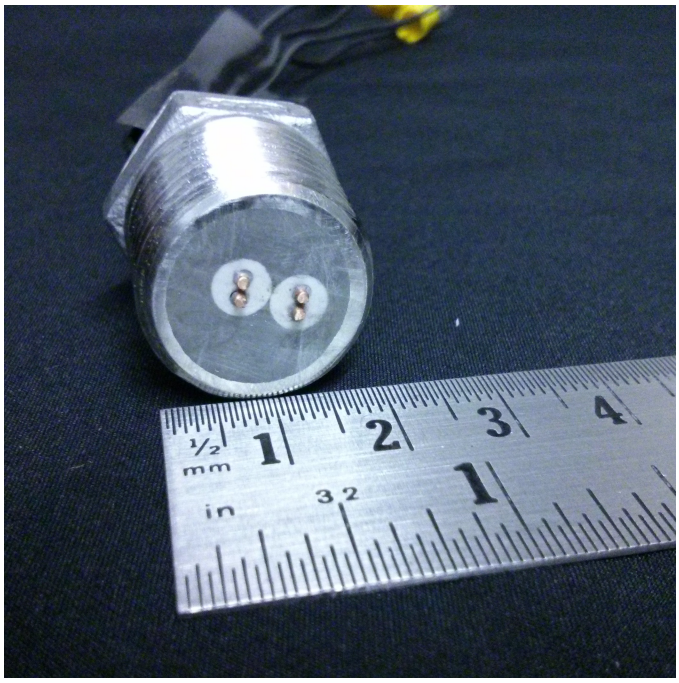

Figure 2.2. Ion gauge.

2.1.3 Testing of Ion Gauge

The ion gauge was tested in a detonation tube as shown in the fig. 2.3. Preliminary tests were conducted on the ion gauge, prior to testing it in the detonation tube. The detonation tube consisted of a 3.5 m long tube, with an internal diameter of 77.9 mm. This tube was connected to a 28.6 mm square duct with an overall length of 1.68 m via a transition section. A Shchelkin spiral was inserted just downstream of the gas injection ports. A mylar diaphragm was used to isolate the detonation tube from the surroundings. The test section which was also a square of 25.4 mm and a length of 305 mm. It was located 150 mm downstream of the transition section. Initially, the tube was evacuated. It was then filled with a stoichiometric oxyhydrogen mixture at one atmosphere using the method of partial pressures. A spark was initiated using a spark plug which is located at the upstream end of the tube. Once

the wave was initiated, the wave traveled downstream through the detonation tube towards the transition section, followed by test section and then finally to the dump tank. The longer duct downstream ensures that the reflection of the wave from the end of the tube does not interfere with the useful test time. An Agilent 6811B AC and DC power supply is used to power the ion gauge circuit.

Figure 2.4 shows the orientation of the sensors placed in the test section. Three PCB Model 111A24 dynamic pressure transducers were used. Two were placed on the either side of the ion gauge and one was placed directly opposite to the ion gauge. Data from the pressure transducers were acquired by an NI PXIe-8130 data acquisition system at 0.5 MHz while the ion gauge data were acquired by a Tektronix DPO 4054 digital storage oscilloscope at 100 MHz.

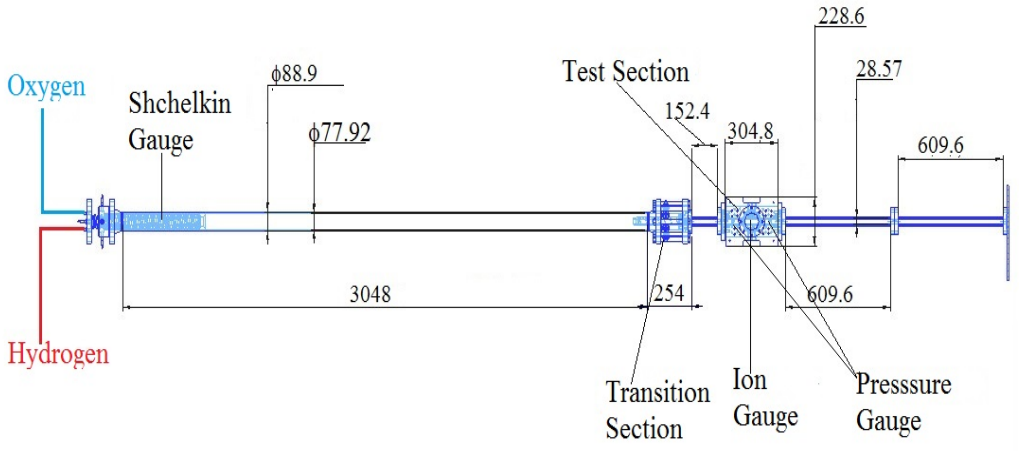

Figure 2.3. Detonation tube (dimensions in mm).

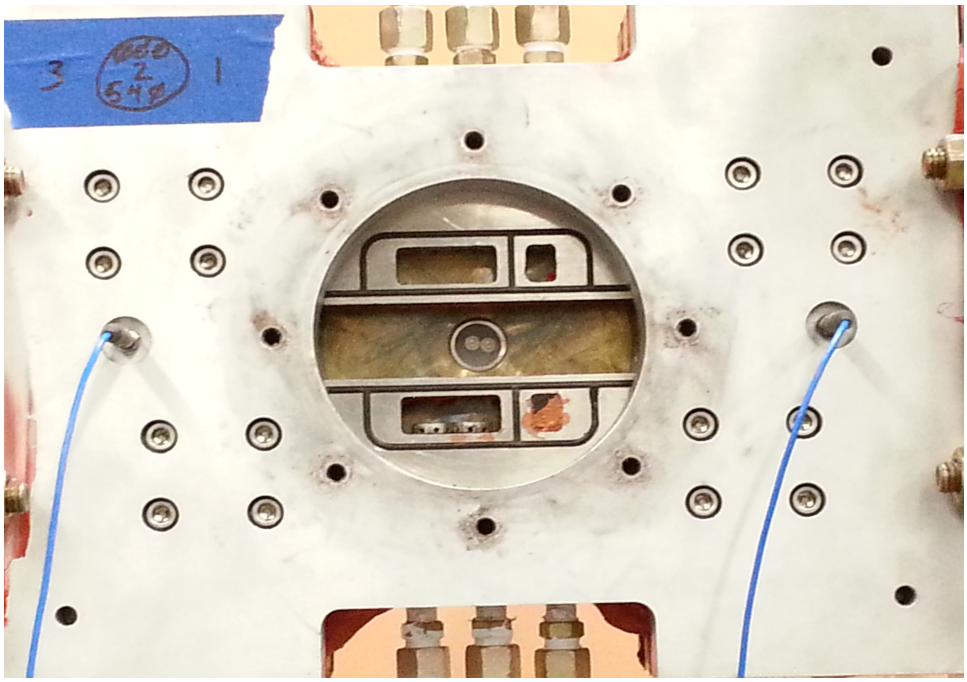

Figure 2.4. Test section showing pressure transducers and ion gauge.

2.2 Detonation Tube

Figure 2.5 shows a panoramic view of the shock-induced detonation tube. From right to left, the tube consists of driver, diaphragm and driven section followed by a dump tank.

Figure 2.5. Panoramic view of shock-induced detonation tube.

The driver tube is made of steel and holds the high-pressure driver gas. It is rated for 6000 psi. The driver section has an internal diameter of 6 inch with 1 inch wall thickness and is 120 inch in length. One end of the driver tube is closed while the other end is connected to a flange which is 19 inch in diameter and 4.5 inch thick. The driver and the diaphragm sections are connected by 8 bolts which are 18 inch in length.

The diaphragm section separates the driver and the driven section. The diaphragm section is made up of three flanges, one connected to driver, one to the driven tube, and third flange is freely supported between the other two by the bolts which connect the sections. In this case, only one side of the diaphragm is used.

The driven or the detonation driven section is filled with a mixture of hydrogen and oxygen. The driven section is comprised of two stainless steel tubes which are 20 ft and 10 ft in length and is 2 inch in diameter. The two tubes are connected by 4 inch diameter flanges.

The dump tank has volume of 150 ft^3 and is placed outside the building. The dump tank possesses a safety valve which opens only due to excess pressure, venting the facility to the atmosphere.

2.2.1 Data Acquisition

PCB111A23 dynamic pressure transducers were used for the detonation tube during operation. Pressure transducers and ion gauges were placed alternatively on the tube. The location of the pressure transducers and ion gauges are shown in the Tables 2.1 and 2.2.

Table 2.1. Position of pressure transducer from the diaphragm

Pressure Transducer	PCB1	PCB2	PCB3	PCB4	PCB5	PCB6
Distance From Diaphragm (ft)	3.5	8.5	13.5	18.5	23.5	28.5

Table 2.2. Position of ion gauge from the diaphragm

Ion Gauge	IG1	IG2	IG3	IG4	IG5
Distance From Diaphragm (ft)	6	11	16	21	26

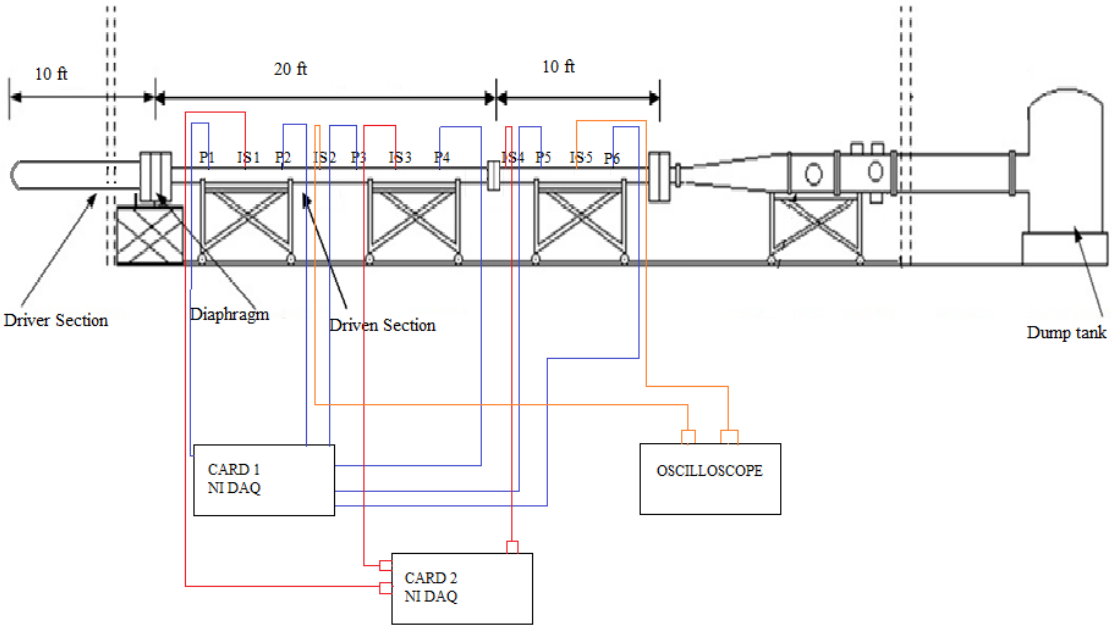

Figure 2.6. Detonation tube with data acquisition.

Figure 2.6 shows the a schematic of the detonation tube and the data acquisition system. The output from the pressure transducers were sent to a National Instruments controller (PXIe-8150) which is indicated with blue lines. This controller holds two TB-2709 data acquisition cards with a total of 16 channels. Six of these channels were used for pressure transducers at a sampling rate of 2 MHz/channel, simultaneous sample-and-hold. The first pressure transducer (closest to the diaphragm section) was used as the trigger for the DAQ.

Three of the five ion gauges, were connected to the DAQ which are indicated in red in fig.2.6. Each ion gauge required two channels and hence six channels were used in the DAQ. Data were acquired at 2 MHz/channel. The remaining two ion gauges (indicated in orange) were connected to the Tektronix DPO 4054 high speed digital storage oscilloscope sampling at 100 MHz/channel.

2.2.2 Detonation Tube Operation

Filling and venting of the tunnel were controlled by pneumatic valves. Air to drive these valves were supplied by a 175 psi compressor. The low-pressure air to control the pneumatic valves is supplied by a Kellogg American Inc. model DB 462-C compressor pump. These pneumatic valves control high-pressure air to the driver and the hydrogen and oxygen bottles for the driven section. The low-pressure air also controls the Haskel pump to be discussed next.

High-pressure air to the driver was supplied from two compressors. A five-stage compressor (Clark Model CMB-6) compressed air to 2100 psi. Air from this initial compressor was sent to a 2-stage Haskel pump where it was compressed to 6000 psi. This high pressure air from the Haskel pump goes to a spherical storage tank which is 1 m in diameter and is rated to 6000 psi.

A mylar diaphragm isolated the driven section from the driver section and another mylar diaphragm was placed at the end of the driven section to contain the test gas from the atmosphere. The driven section was evacuated a HyVac vacuum pump. A static pressure transducer (Omegadyne PX209-100A5V) was to used to measure the vacuum in the driven tube. Industrial hydrogen and oxygen bottles rated at 2200 psi supply the detonation tube.

To start the test, the driven section was first evacuated to 0.01 atm using the vacuum pump. Hydrogen was then pumped into the driven section followed by oxygen to achieve a stoichiometric mixture at a set initial pressure. This mixture was left for 10 minutes to ensure that proper mixing is achieved in the section. To initiate the test, high pressure air from the spherical tank was fed to the driver section. The diaphragm at the diaphragm section ruptured when a certain pressure was reached in the driver section thereby releasing a normal shock wave into the driven section and simultaneously releasing an expansion wave into the driver section. The normal shock

transitioned into a detonation wave and the wave propagated through the driven tube. The detonation wave then rupture the mylar diaphragm at the end of the driven tube before entering into the dump tank.

CHAPTER 3

RESULTS AND DISCUSSION

Discussion of the test results is divided into two sections. The first part describes the testing of the ion gauge and the second part describes using ion gauges to study the propagation of a detonation wave.

3.1 Results of Ion Gauge Testing

The outputs from the pressure transducers and ion gauges are shown in figs.3.1 and 3.2 respectively. Figure3.1(a) shows the sharp pressure peaks followed by the Taylor expansion. The pressure peak has been zoomed in fig.3.1(b). Figure3.2(b) shows the zoomed-in peaks from the charge buildup and discharge of the free radicals as the combustion zone of the detonation wave transits each pair of electrodes.

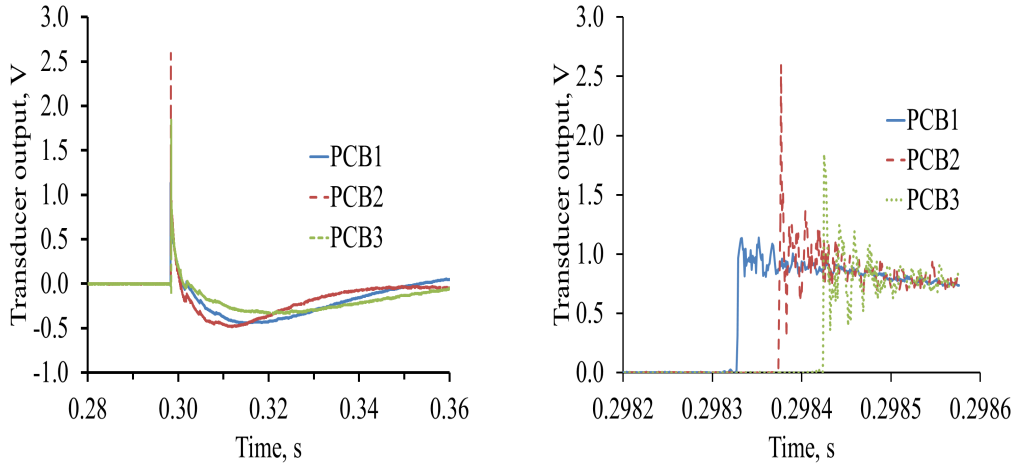

(a) Signals

(b) Enlargement of 3.1(a)

Figure 3.1. Pressure transducer outputs.

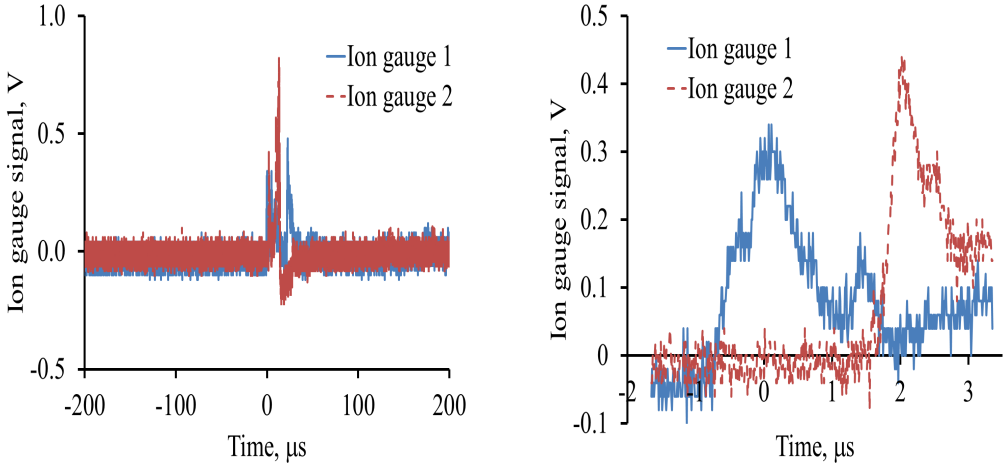

(a) Signals

(b) Enlargement of 3.2(a)

Figure 3.2. Ion gauge outputs.

Non-stationary cross correlation was applied to data obtained from the pressure transducers and ion gauges. Figure3.3 shows the plot for cross correlation which represent the time delay between the two peaks. Data that exceeded some threshold limit were excluded as shown in fig.3.3(a). The standard deviation was used as the measure of uncertainty.

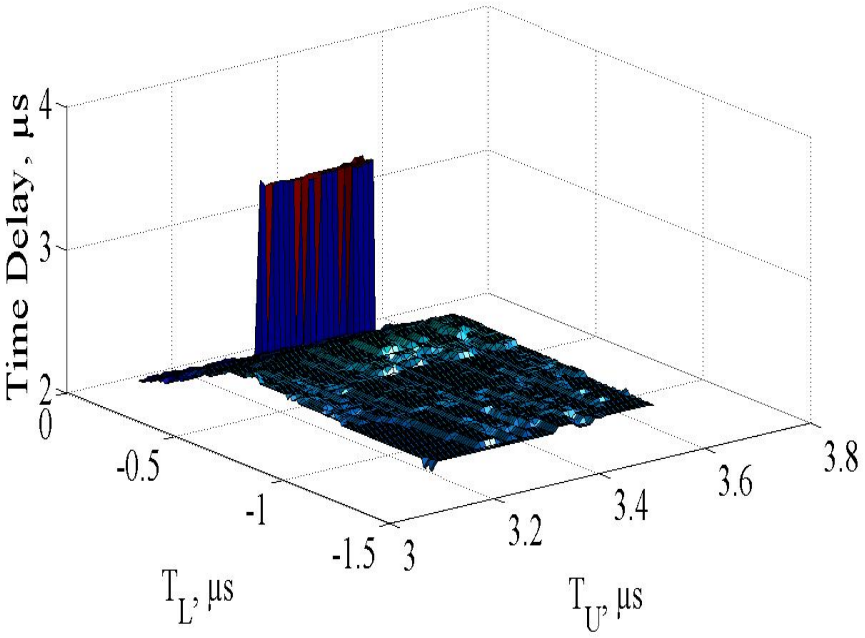

(a) Signals

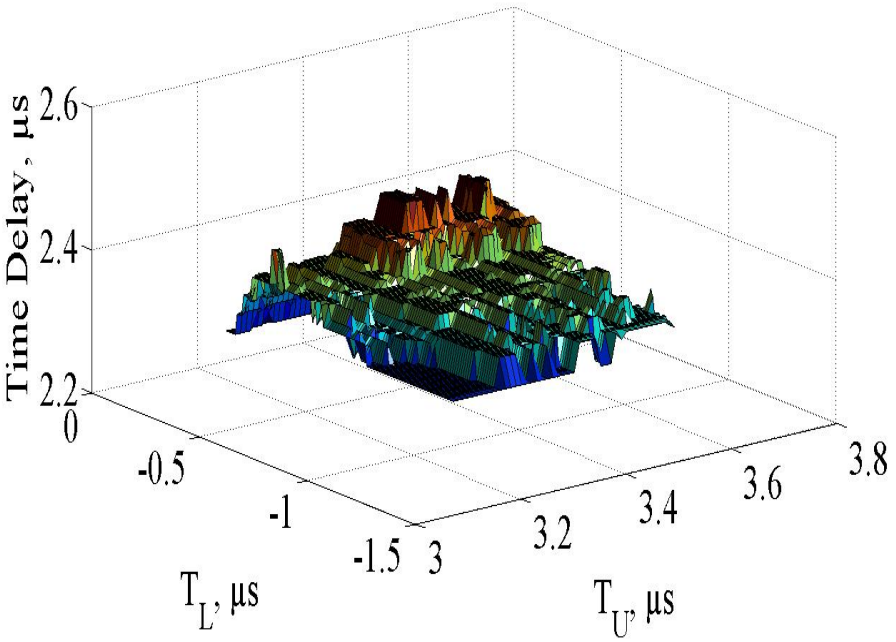

(b) Enlargement of 3.3(a)

Figure 3.3. Nonstationary cross-correlation of the ion gauge.

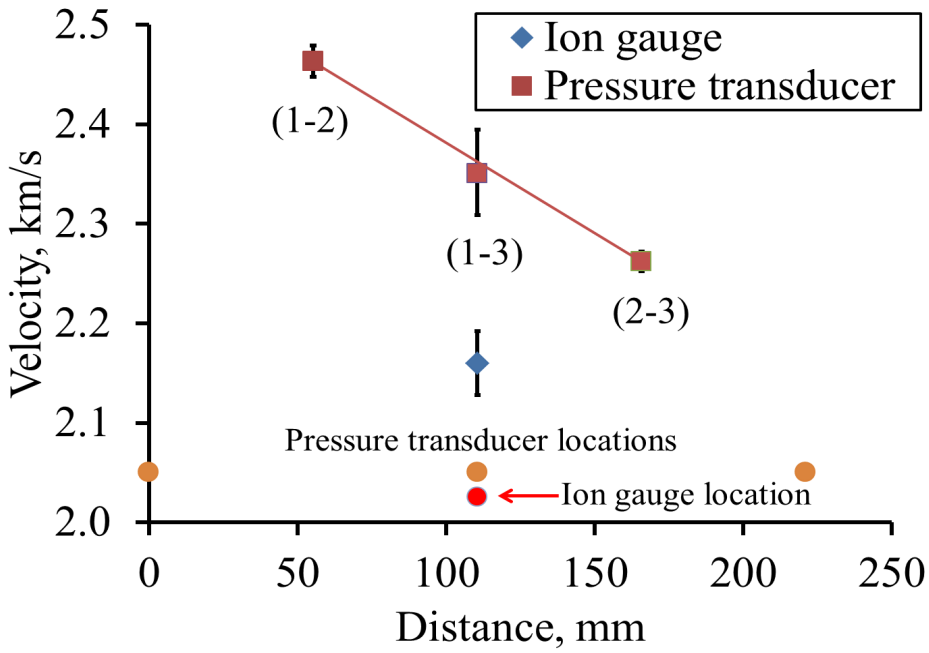

Figure 3.4. Propagating velocities of detonation wave.

Figure 3.4 shows the detonation wave propagation velocity measured by the pressure transducers (time-of-flight) and ion gauge (point measurement). It can be seen from the plot that the propagation velocity measured by the pressure transducers reduced from 2.46 to 2.26 km/s whereas the velocity obtained from the ion gauge was around 2.16 km/s.

3.2 Results from Detonation Tube

The analysis for the detonation tube is similar to that of Bello [10]. Knowing the fuel-oxidizer ratio, initial pre-detonation pressure and initial temperature, the online NASA CEA code was used to determine the detonation wave parameters via the 'det' option [11]. The post-detonation wave properties include the burned gas

pressure (p_{CJ}), temperature (T_{CJ}), density (ρ_{CJ}), gas sonic velocity (a_{CJ}), detonation wave velocity (u_{CJ}) and Mach number (M_{det}).

3.2.1 Results from NASA CEA Code

All tests were performed with the driver pressure at 45 atm and 300 K. The pre-detonation pressure is set at either 2 atm or 3 atm, giving P_4/P_1 pressure ratios of 22.5 and 15, respectively. Results for these conditions are shown in the table 3.1

Table 3.1. Theoretical values for detonation tube

Pre-detonation pressure	2 (atm)	3 (atm)
Initial temperature	300	300
p_{CJ}(atm)	38.27	58.89
u_{CJ}(m/s)	2873	2895
ρ_{CJ}(kg/m^3)	1.79	2.68
T_{CJ}(K)	3809	3889
a_{CJ}(m/s)	1564	1577

3.2.2 Experimental Results

Experimental results for shock-induced detonation were obtained for pre-detonation pressures of 2 and 3 atm. The pressure traces for PCB's mounted along the tube and the ion gauge traces show similar characteristics for 2 atm and 3 atm. Hence, pressure and ion gague trace plots are shown only for 3 atm.

Figure 3.5 shows the PCB pressure traces for 3 atm pre-detonation pressure. It can be seen that there are a lot of fluctuations at the PCB1 location. These fluctuations remained even after the pressure transducers were interchanged. These fluctuations were also seen for other shock-induced detonation tests as well. Figure 3.6 show the output for ion gauges 1, 3 and 4. IG11 and IG12 depicts the first and

second probes of ion gauge 1. Figure 3.7 represents the ion gauge outputs for 2 and 5 and fig.3.7(b) represents the zoomed-in version of ion gauge 2.

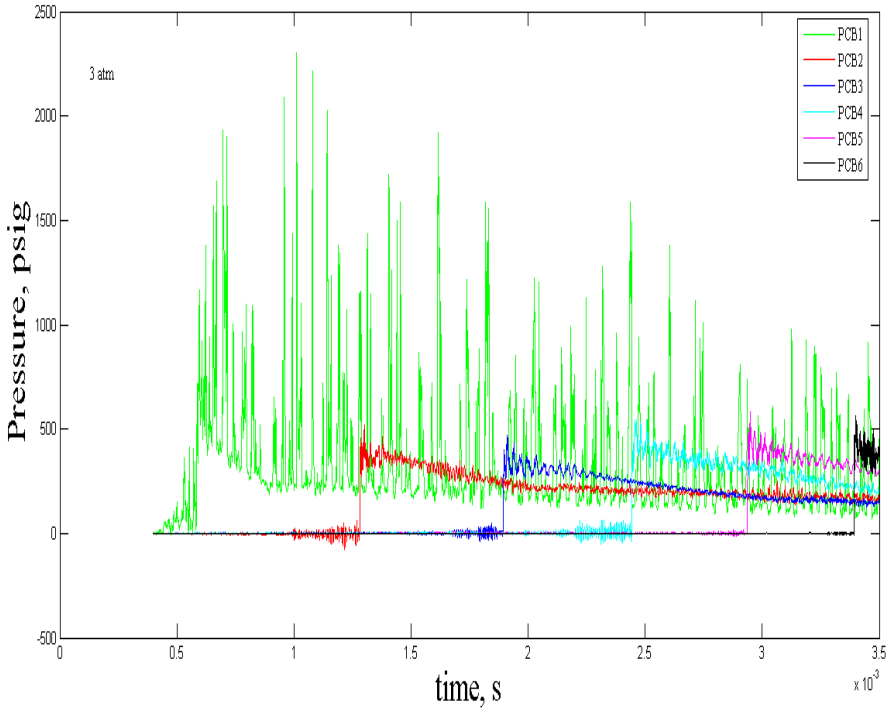

Figure 3.5. PCB pressure output for 3 atm.

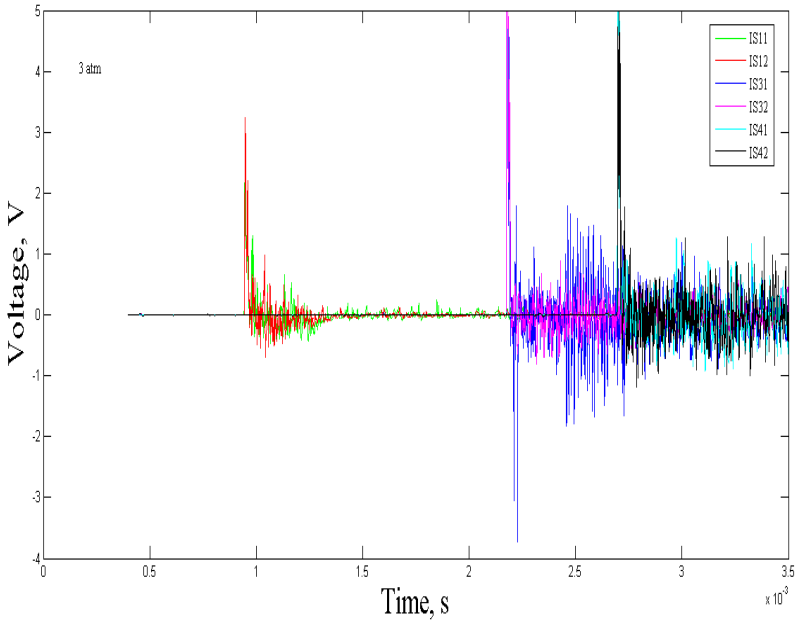

Figure 3.6. Ion gauge output for 3 atm .

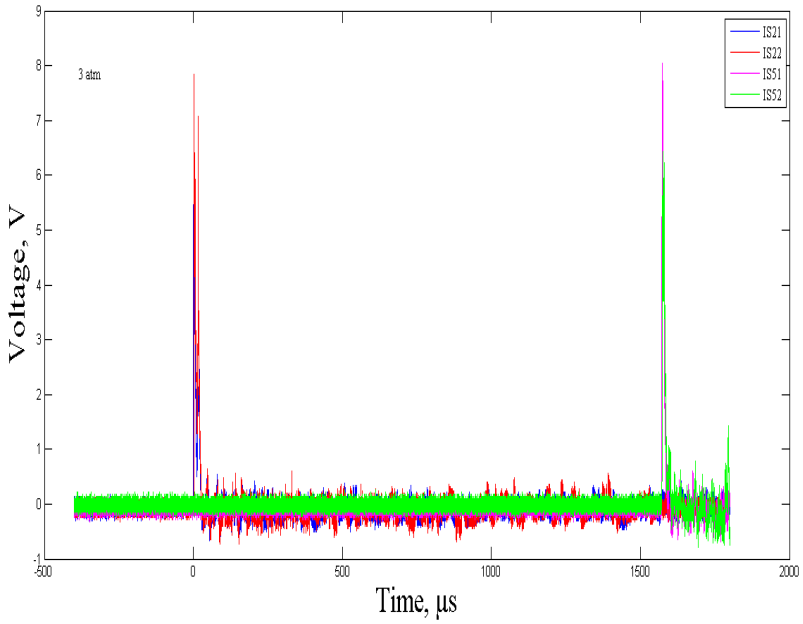

(a) Signals

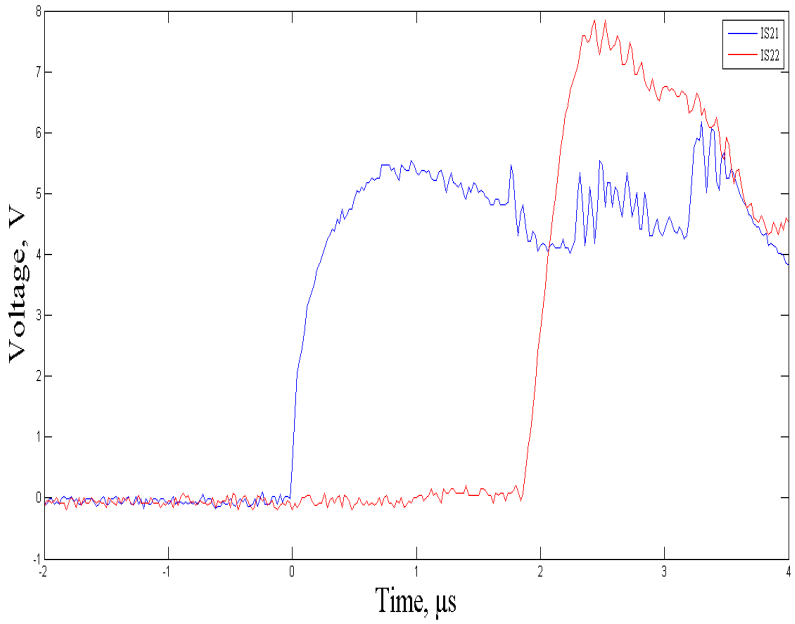

(b) Enlargement of 3.3(a)

Figure 3.7. Ion gauge output from oscilloscope.

A non-stationary cross-correlation technique is applied to these outputs to find the velocities and their uncertainties for pressure transducers and ion gagues. Cross-correlation plots for all the ion gauges and pressure transducers have similar characteristics; therefore, fig.3.8 shows a sample cross-correlation plot for the second ion gauge.

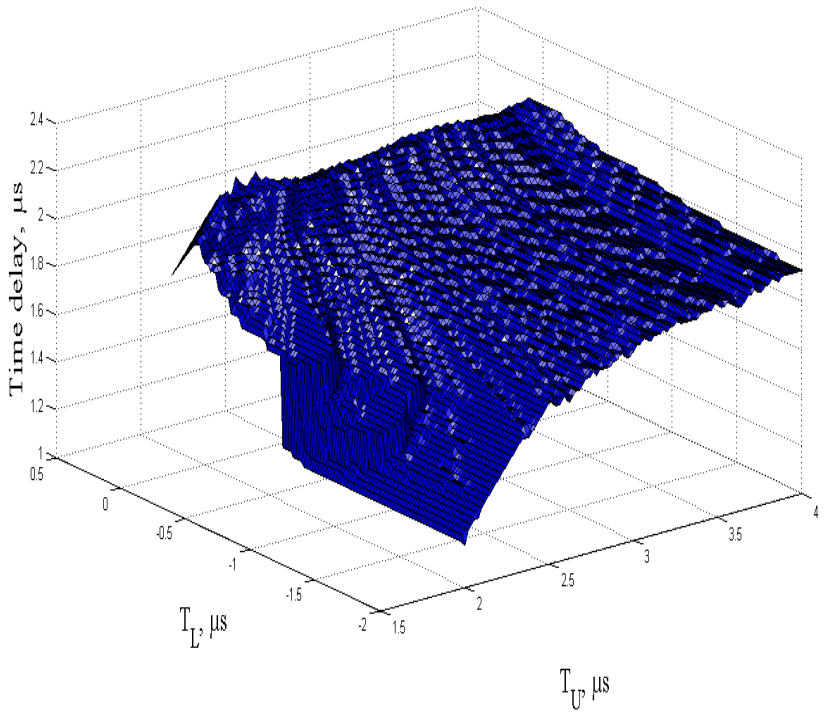

Figure 3.8. Cross correlation plot for ion gauge 2 .

Figures 3.9 and 3.10 show the velocities with respect to the distance from the diaphragm. The red line indicates the velocity for the ion gauges and the green line indicates the velocity profile for PCB. u_{CJ} indicates the CJ velocity for the detonation wave. The plots indicate that the velocity increases downstream of the ignition source.

Figure 3.11 shows the plot of repeatability for 2 atm pre-detonation pressure and the trend remains the same. The velocity still increases downstream of the ignition source.

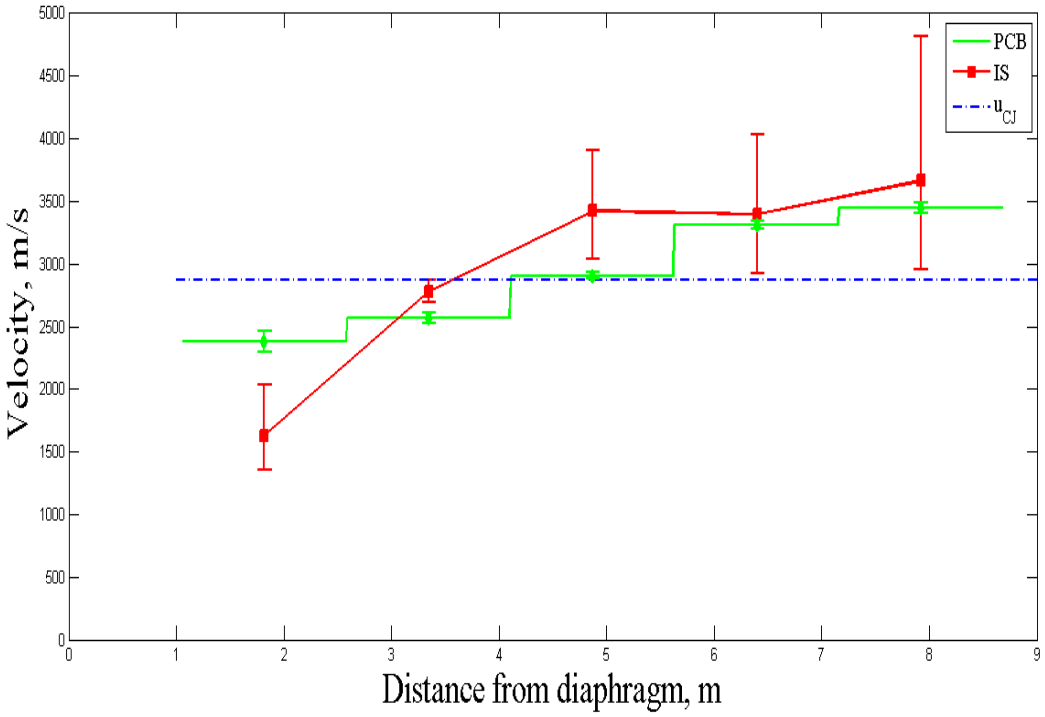

Figure 3.9. Velocity profile for 2 atm.

3.2.3 Shock Tube Experiments

Results for shock tube experiments that were conducted to provide a comparison between detonation wave and shock wave propagation behavior are discussed in this section. The shock tube experiments were performed for 2 and 3 atm driven pressure with an air driver initially at 45 atm and 300 K. Figure 3.12 shows the traces from the pressure transducers mounted along the tube for 2 atm only as 2 and 3 atm show similar charateristics. Figures 3.13 and 3.14 show the plots for the 2 and 3

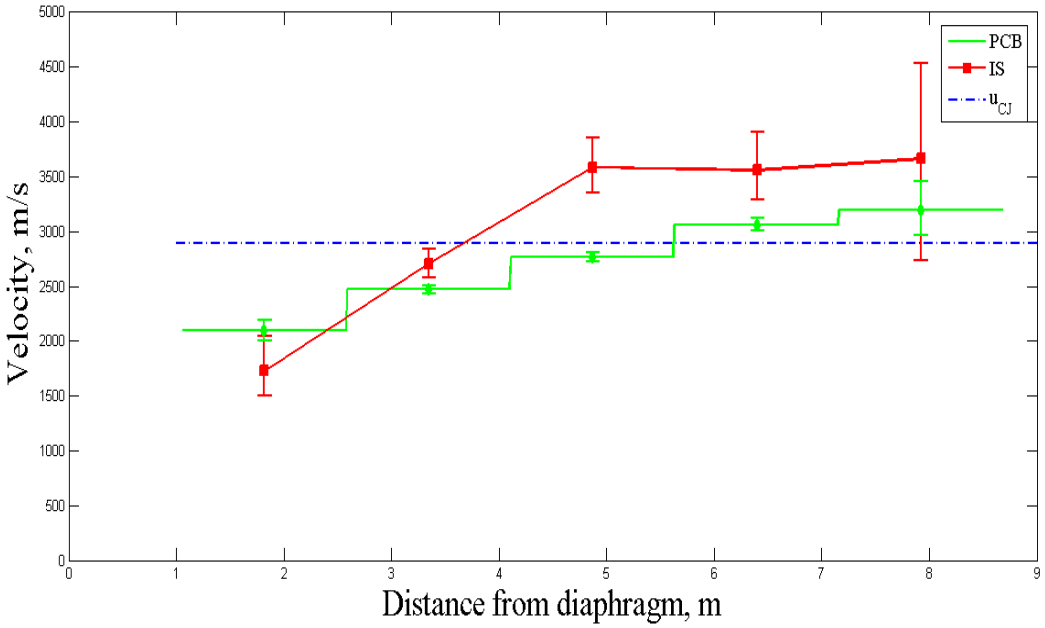

Figure 3.10. Velocity profile for 3 atm.

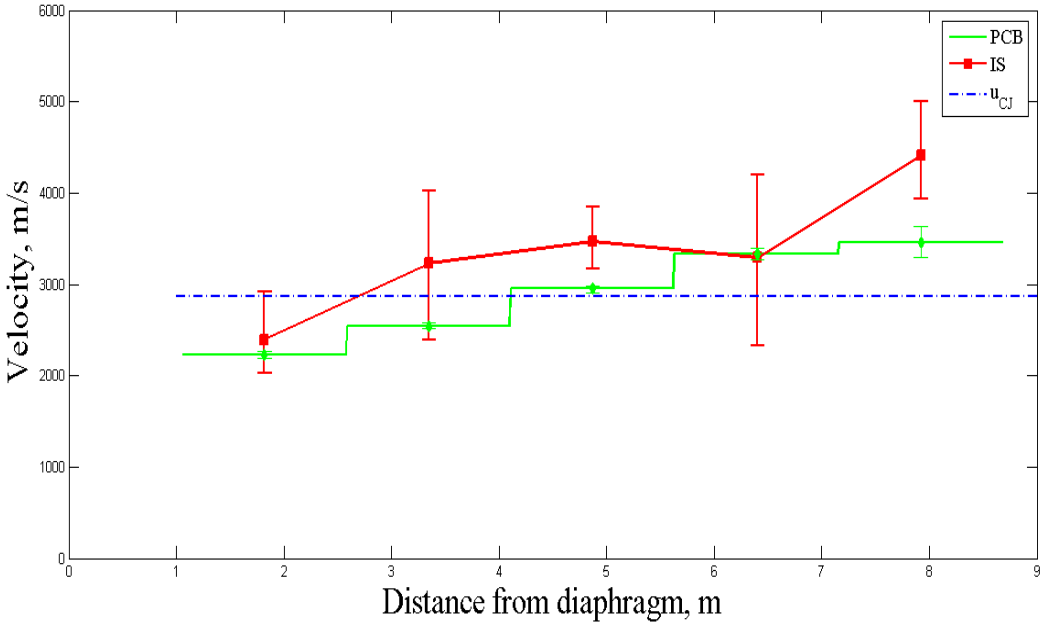

Figure 3.11. Velocity profile for 2 atm (repeatability).

atm driven pressure tests respectively. The plots show velocity obtained by pressure transducers. It can be seen that the shock wave velocity attenuates as the wave propagates downstream from the diaphragm. The theoretical velocity was indicated using the blue dotted line. This theoretical value is calculated using the NASA CEA online code by choosing the shock option. This code also provides the theoretical P_2/P_1 value.

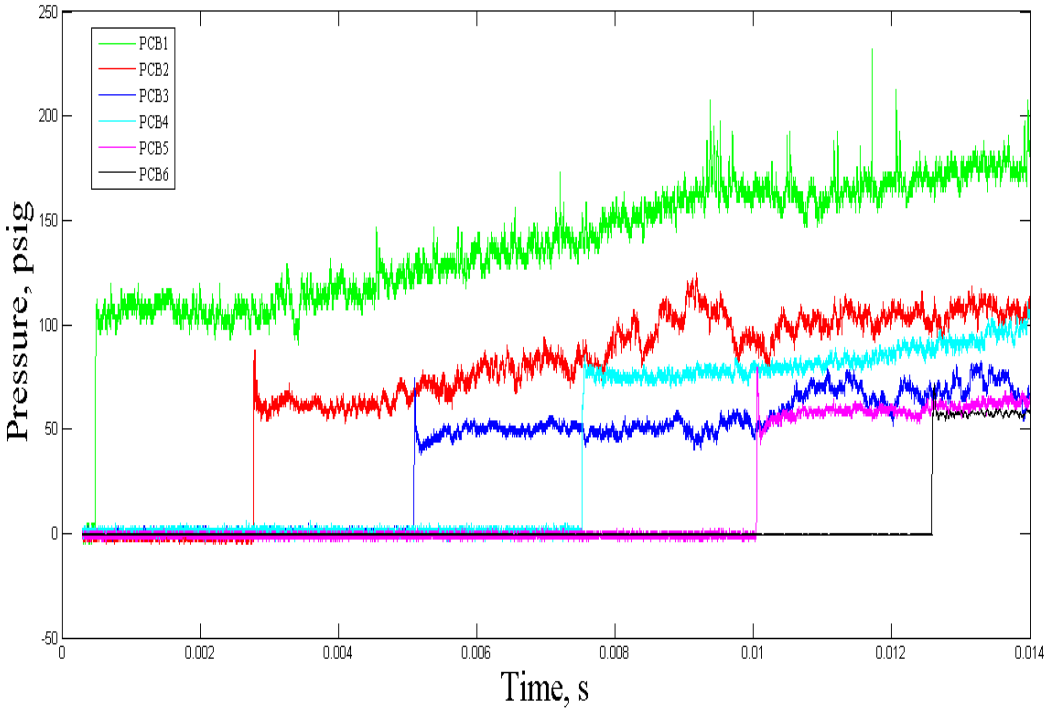

Figure 3.12. PCB pressure output for 2 atm .

Figures 3.15 and 3.16 show P_2/P_1 with respect to the distance from the diaphragm. The blue curve indicates the theoretical value. The green curve indicates P_2/P_1 calculated using the instantaneous Mach number at different locations of the tube. Both the red and pink curves indicates the P_2/P_1 determined from the PCB

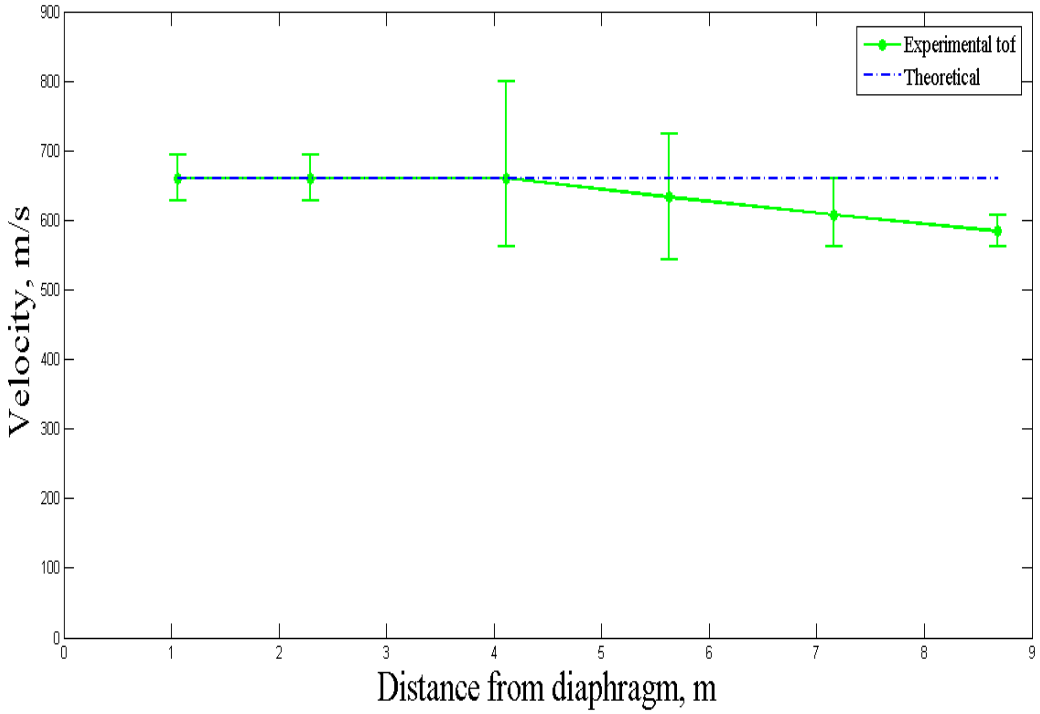

Figure 3.13. Velocity from pressure transducer for 2 atm .

pressure transducers. The red curve indicates the mean value of P_2 whereas the dark green curve indicates the peak P_2 value from the PCB pressure transducers. The plots reveal that the pressure behind the shock wave also attenuates downstream from the diaphragm. The plots also reveal that the pressure ratio increases for the fourth pressure transducer and reduces again. A Faulty pressure transducer might be the probable reason for the pressure increase.

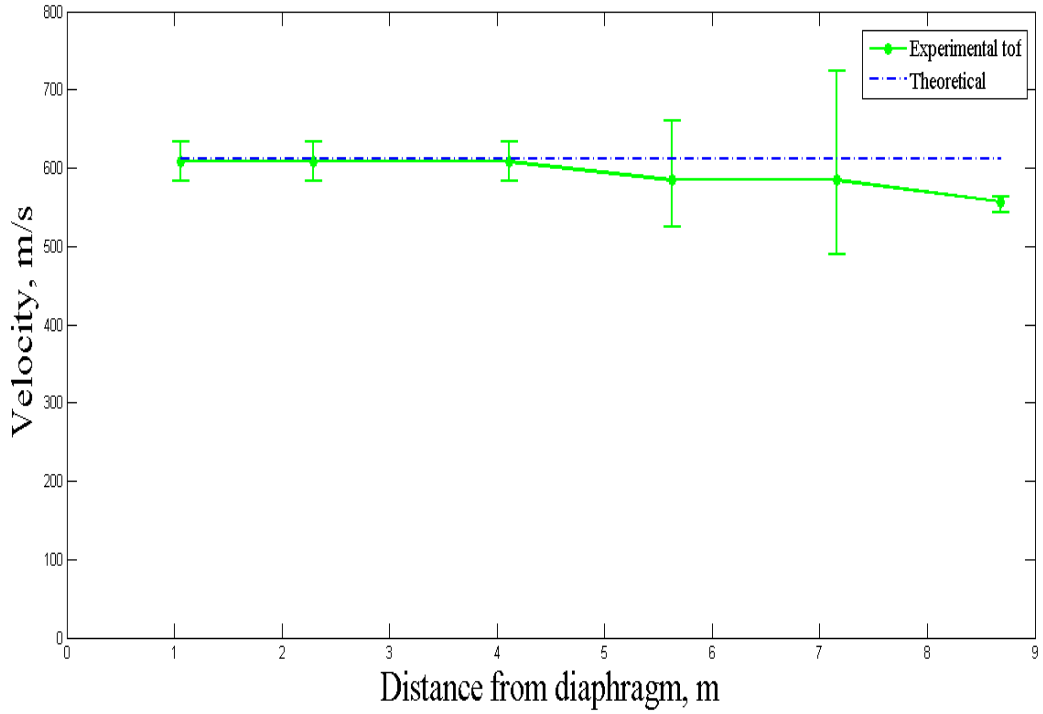

Figure 3.14. Velocity from pressure transducer for 3 atm .

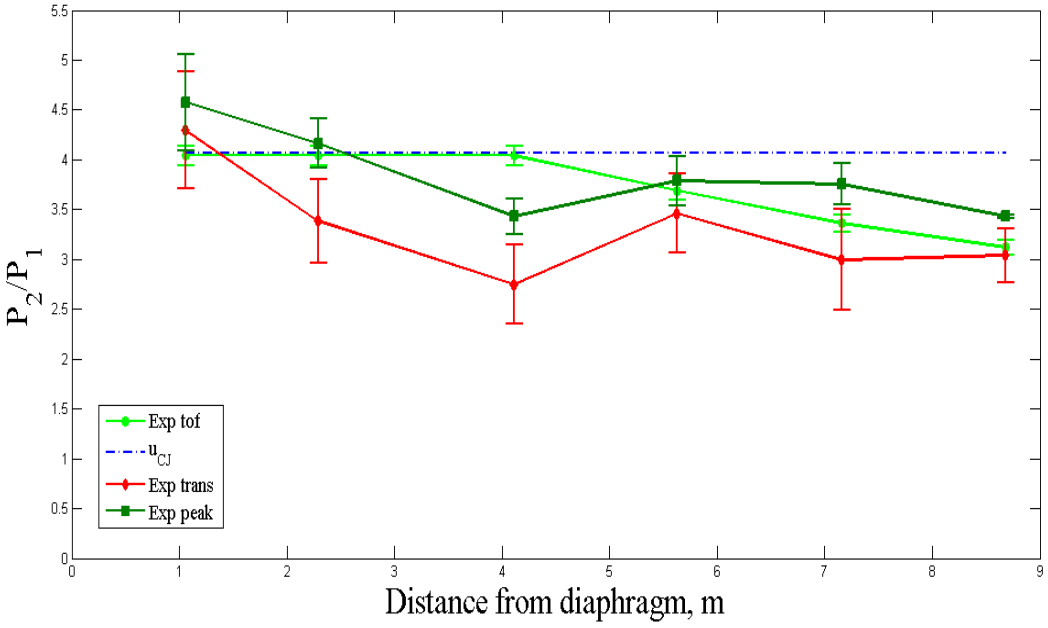

Figure 3.15. Pressure ratio along the tube for 2 atm .

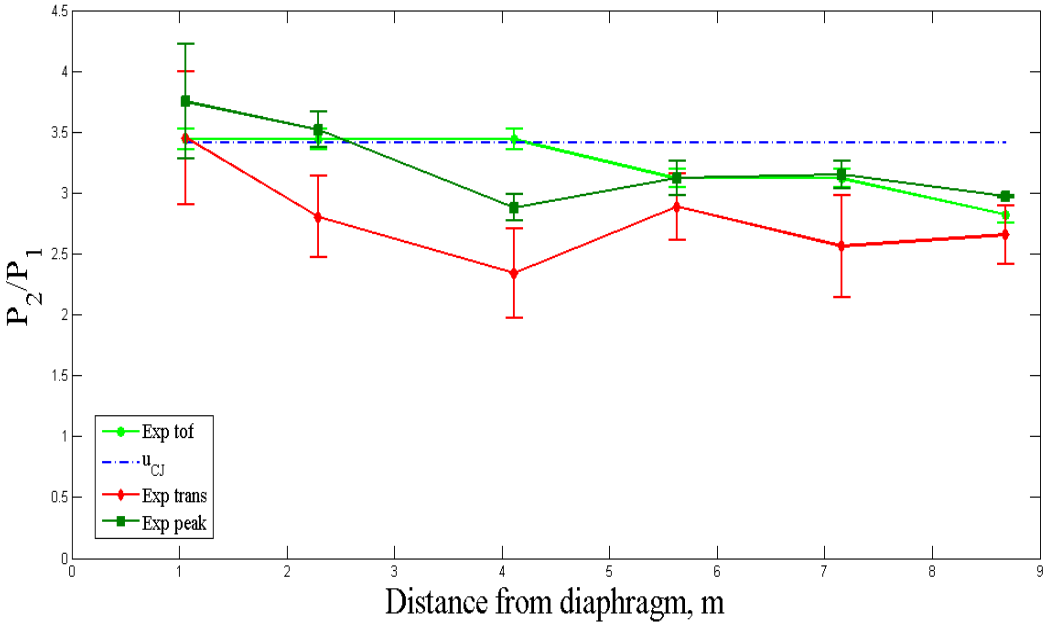

Figure 3.16. Pressure ratio along the tube for 3 atm .

Figures 3.17 and 3.18 shows the ratio of instantaneous P_2 to the initial P_2i(pressure behind the shock wave) versus the distance from the diaphragm. The blue and the red curves are the curves obtained from Mirel's theory for laminar and turbulent case [12]. The dashed blue and red curves indicate the extrapolated values of the Mirel's theory. The green curve indicates the experimental values determined by the time-of-flight method. The pink curve indicated the values obtained from the pressure transducers. It can be seen from the plots that the shock wave follows laminar trend till 4 m and then it follows the turbulent trend.

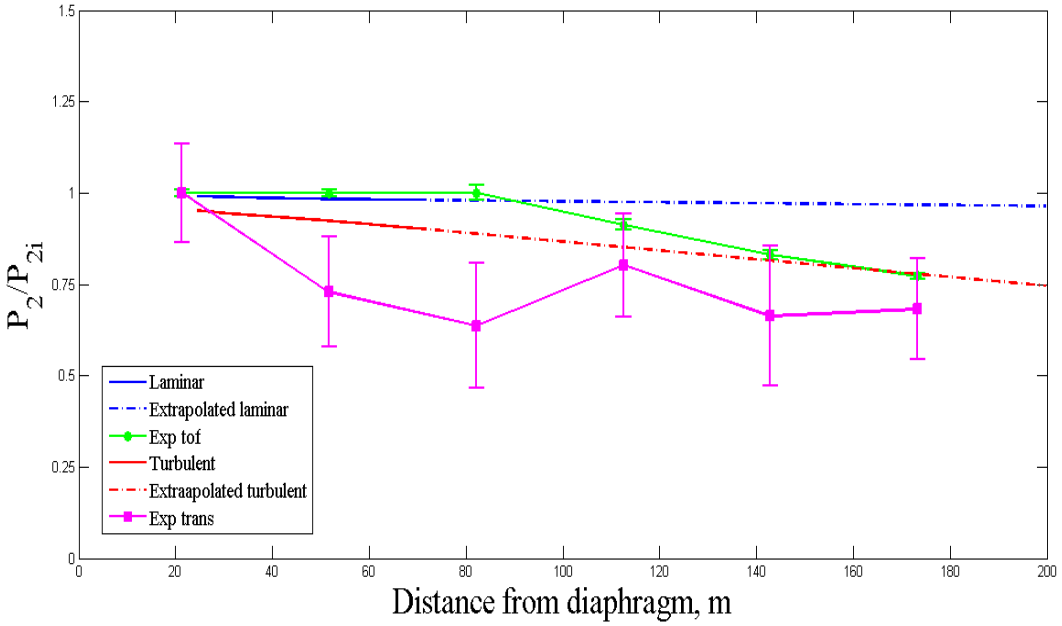

Figure 3.17. Comparison with Mirel's theory for 2 atm .

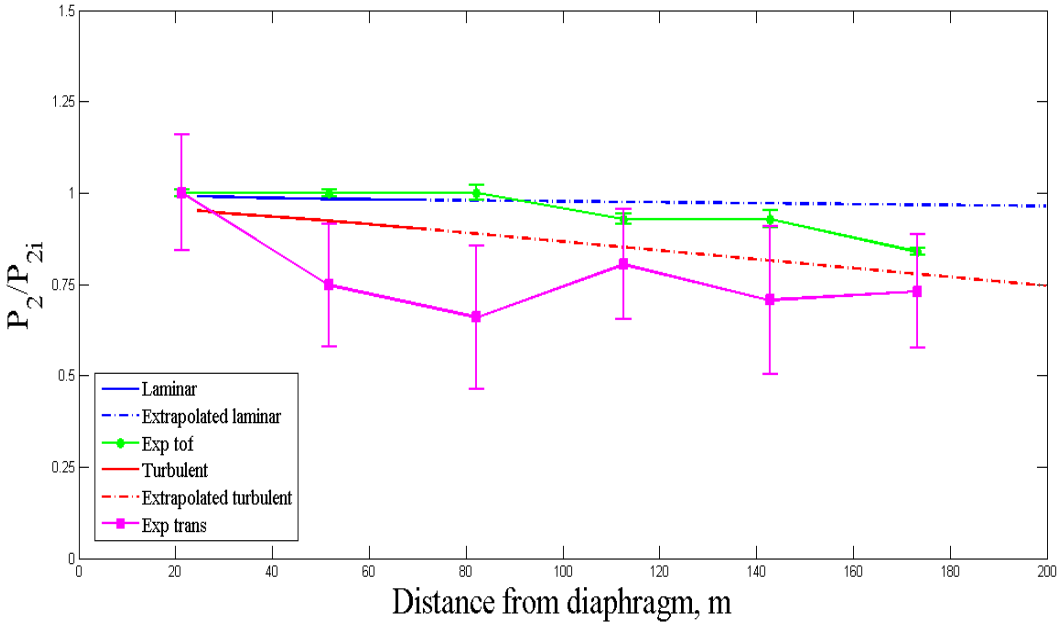

Figure 3.18. Comparison with Mirel's theory for 3 atm .

CHAPTER 4

CONCLUSIONS AND FUTURE WORK

4.1 Conclusions

A closely-spaced pair of ion gauges was built into a single plug. The ion gauges successfully detected the passage of detonation wave. A non-stationary cross-correlation technique was used to obtain the velocity and its uncertainty.

The velocity in the first detonation tube was lower than CJ velocity because the area of cross-section of the tube reduced after the transition section. This was not seen in the shock-induced detonation tube since the cross-sectional area of that tube was uniform. Experimental tests were conducted for pre-detonation pressure at 2 and 3 atm. The velocity of the detonation wave in the shock-induced detonation tube increases downstream of the diaphragm due to the continuous supply of combustible mixture, which overcomes the attenuation effects such as friction and boundary layer buildup. On the other hand, velocity of a shock wave attenuates downstream of the diaphragm due to friction and the boundary layer buildup. Pressure behind the shock is compared qualitatively to that with of Mirel's laminar and turbulent theory and they follow the same trend.

4.2 Future Work

Electrodes of the ion gauge can be much thinner making the design more compact. Currently, the electrodes are not flushmounted which make it prone to bending due to repeated tests. Flushmounting of the electrodes will negate the possibility of bending and erosion. Wavelet transformations can be used to determine the velocity

and the uncertainty. Data from the ion gauges can be multiplexed so that it samples at high frequency. Detonation experiments can be carried out on a much smaller diameter tube so that the boundary layer growth and the attenuation behavior can be understood.

APPENDIX A

Cross Correlation Code

In this appendix, matlab program used for cross correlation technique is shown.

```
clear all; clc; close all;
    ab = 2*400;
    bc = 2*3500;
    M = dlmread('daq3nov2t.lvm','',24,0);
    t = M(ab:bc,1);
    t(2:2:end) = t(2:2:end) + 0.0000005;
    tt = t*10^6;
    PCB1 = M(ab:bc,2)/0.0005;
    PCB2 = M(ab:bc,3)/0.0005;
    PCB3 = M(ab:bc,4)/0.0005;
    PCB4 = M(ab:bc,5)/0.0005;
    PCB5 = M(ab:bc,6)/0.0005;
    PCB6 = M(ab:bc,7)/0.005;
    Ion11 = M(ab:bc,8);
    Ion12 = M(ab:bc,9);
    Ion31 = M(ab:bc,10);
    Ion32 = M(ab:bc,11);
    Ion41 = M(ab:bc,12);
    Ion42 = M(ab:bc,13);
    figure (2)
    plot(t,Ion11,'g');
    hold on
    plot(t,Ion12,'r');
    hold on
    plot(t,Ion31,'b');
```

```
hold on
plot(t,Ion32,'m');
hold on
plot(t,Ion41,'c');
hold on
plot(t,Ion42,'k');
hold off
i = 1; inde = 1;
a = [];b = []; main = [];
is = [];js = [];ti = [];
avg = [];plus = [];ais = [];
while Ion41(i)¡ max(Ion41)
j = length(Ion42);
tj = [];
while Ion42(j)¿0.1
NC1 = Ion41(i:j);
NC2 = Ion42(i:j);
[Rxy,lag] = xcorr(NC2,NC1,'unbiased');
[m ,ind] = max(Rxy);
tdelayest2 = lag(ind)*((t(end)-t(1))/length(t));
b = [b tdelayest2];
clear NC1 NC2 xcf;
js = [js t(j)];
is = [is t(i)];
tj = [tj t(j)];
j = j-1;
```

```
end
std1 = std(b);
var1 = var(b);
alpha = .05;
mean1 = mean(b);
ais = [ais i];
plot3(js,is,b);
hold on;
a(inde,:) = b;
main = [main b];
inde = inde+1;
ti = [ti t(i)];
is = [];js = [];
b = [];
i = i+1;
end
hold off
figure(5);
surf(tj,ti,a,'FaceColor','blue','EdgeColor','none');
mainAvg = mean(main)
mainStd = std(main);
up = mainAvg+mainStd
down = mainAvg-mainStd
mainConfInt = norminv(.05,mainAvg,mainStd)-mainAvg;
hold off
figure(3);
```

```
errorbar(1,mainAvg,mainStd,'*');
```

REFERENCES

[1] F. Lu, A. Ortiz, J.-M. Li, C. Kim, and K.-M. Chung, "Detection of shock and detonation wave propagation by cross correlation," *Mechanical Systems and Signal Processing*, vol. 23, no. 4, pp. 1098 – 1111, 2009.

[2] R. F. Flagg, "Ionization gauge circuit for detection of multiple shock and reflected detonation waves," *Review of Scientific Instruments*, vol. 38, no. 9, pp. 1336–1337, 1967.

[3] L. Bollinger, "Experimental detonation velocities and induction distances in hydrogen-air mixtures," *AIAA Journal*, vol. 2, no. 1, pp. 131–133, 1964.

[4] J. Skinner, "Friction and heat-transfer effects on the nonsteady flow behind a detonation," *AIAA Journal*, vol. 5, no. 11, pp. 2069–2071, 1967.

[5] J. Angelone, "Shock tube: High temperature gas dynamic studies," *Master's Thesis, Department of Aerospace Engineering, University of Texas at Arlington*, 1978.

[6] I. Glassman and R. Yetter, "Combustion," *Elsevier Science*, 2008.

[7] F. Lu and A. Ortiz, "Wavelets for uncertainty estimates of propagating shock and detonation waves," *Experiments in Fluids*, vol. 52, no. 1, pp. 167–178, 2012.

[8] A. Ortiz and F. Lu, "Correlation and spectral methods for determining uncertainty in propagating discontinuities," *Signal Processing, IEEE Transactions on*, vol. 58, no. 5, pp. 2494–2508, 2010.

[9] H. T. Knight and R. E. Duff, "Precision measurement of detonation and strong shock velocity in gases," *Review of Scientific Instruments*, vol. 26, no. 3, 1955.

[10] R. Bello, "High-enthalpy characteristics of the uta hypersonic shock tunnel," *Master's Thesis, Department of Aerospace Engineering, University of Texas at Arlington*, 2012.

[11] D. M. J. Zehe. (2012) Cearun ed. [Online]. Available: http://cearun.grc.nasa.gov/

[12] H. Mirels and U. S. N. A. C. for Aeronautics, *Attenuation in a Shock Tube Due to Unsteady-boundary-layer Action*, ser. Technical note. National Advisory Committee for Aeronautics, 1954.

BIOGRAPHICAL STATEMENT

Nitesh Karpakala Manjunatha Gupta was born in Chinthamani, Karnataka, India in 1989. He received his Bachelors in Engineering in Mechanical Engineering from Global Academy of Technology (a part of Visvesvaraiah Technological University). He worked as a summer intern at Bosch, Bangalore, in 2009. He has been a part of the Aerodynamics Research Center at the University of Texas at Arlington since 2011. His research interest includes hypersonic shock tunnels, detonation tubes and aerodynamics.